

Stabilization of Bose-Bose mixtures on a spherical surface induced by the Lee-Huang-Yang correction

Wen-Hao Li, Ming Gong,^{*} Zheng-Wei Zhou^{✉,†} and Xiang-Fa Zhou^{✉,‡}

CAS Key Laboratory of Quantum Information and Anhui Center for Fundamental Sciences in Theoretical Physics, University of Science and Technology of China, Hefei, Anhui 230026, China;

Synergetic Innovation Center of Quantum Information and Quantum Physics, University of Science and Technology of China, Hefei, Anhui 230026, China;

and Hefei National Laboratory, University of Science and Technology of China, Hefei, Anhui 230088, China



(Received 24 December 2024; accepted 14 March 2025; published 1 April 2025)

Motivated by recent experimental advances in bubble traps which confine atoms on a thin shell, we investigate the stabilization of droplet states of a Bose-Bose mixture on a spherical surface due to quantum fluctuations. We analytically calculate the energy of a weakly interacting Bose-Bose mixture on a spherical surface with attractive interspecies and repulsive intraspecies interactions using the Bogoliubov approximation. Our findings show that the energy per particle has a minimum at a finite density in the presence of the Lee-Huang-Yang (LHY) term, which indicates the presence of liquidlike droplet state stabilized by quantum fluctuations. We also numerically solve the extended Gross-Pitaevskii equation, incorporating both bubble traps and an additional repulsive LHY correction derived from the Bogoliubov spectrum of a three-dimensional homogeneous mixture. Our calculations show that, due to the size limitations of the sphere, droplet states can only exist within specific parameter ranges. We also verify the transition between droplet states and uniform condensates in spherical confinement potentials, as well as the coexistence of the two. Our results pave the way for future exploration of quantum droplets in curved geometries with nontrivial real-space topologies.

DOI: [10.1103/PhysRevA.111.043301](https://doi.org/10.1103/PhysRevA.111.043301)

I. INTRODUCTION

Since the physical realization of ultracold quantum gases, exploring the various exotic quantum states caused by interactions in cold atoms has continuously been an important issue of significant interest in both theoretical and experimental research. Although in most cases the conclusions obtained from the mean-field method have been well matched with experimental results [1–4], there are also many experiments that show that fluctuations beyond the mean field can lead to observable physical effects, resulting in new quantum phases. Theoretically, Lee *et al.* provided the ground-state energy density of a homogeneous weakly repulsive Bose gas, including the mean-field term and the first beyond-mean-field contribution, known as the famous Lee-Huang-Yang (LHY) correction [1],

$$\epsilon_{\text{MF}} + \epsilon_{\text{LHY}} = \frac{gn^2}{2} \left[1 + \frac{128}{15} \left(\frac{a^3 n}{\pi} \right)^{1/2} \right], \quad (1)$$

where a is the s -wave scattering length, g is the interaction coupling constant, and n is the particle-number density. In the weak-interaction regime with $n|a|^3 \ll 1$ [5], the LHY correction due to quantum fluctuations is indeed small compared to the mean-field term, which thus can be safely neglected in most cases. Due to recent advancements in experimental

techniques and the application of Feshbach resonance in the field of cold atoms, researchers have succeeded in observing the effects induced by the LHY correction in some ultracold atomic experiments [6]. However, the more significant observable physical effects caused by the LHY correction remain to be explored.

Fortunately, for a Bose-Bose mixture, Petrov found that the LHY correction can be dominant and leads to the formation of stable quantum droplet states in such a dilute weak-interaction systems [7]. Physically, according to mean-field theory, the stability condition for a Bose-Bose mixture can be expressed as [8]

$$g_{11} > 0, \quad g_{22} > 0, \quad g_{11}g_{22} > g_{12}^2, \quad (2)$$

where g_{ii} ($i = 1, 2$) and g_{12} represent the intra- and interspecies coupling constants, respectively. If the Bose-Bose mixture supports weak interspecies attractive and intraspecies repulsive interactions, characterized by $g_{12} < 0$, $g_{11} > 0$, and $g_{22} > 0$, then according to mean-field theory, the ground-state energy density $\epsilon_{\text{MF}} \propto n^2$ can be negative if $\delta g = g_{12} + \sqrt{g_{11}g_{22}}$ is slightly less than zero. Therefore, naively, one may think that the system will gradually collapse due to the effective attractive interaction. However, since the mean-field term and the LHY term have different dependences on the inter- and intraspecies coupling constants ($\epsilon_{\text{LHY}} \propto n^{5/2}$) and can be independently controlled under weak-interaction conditions [7], this implies that the repulsive force provided by quantum fluctuations can offset the attractive force corresponding to the mean-field predicts. Thus, the Bose-Bose mixture does not collapse as described by mean-field theory

^{*}Contact author: gmgong@ustc.edu.cn

[†]Contact author: zwzhou@ustc.edu.cn

[‡]Contact author: xfzhou@ustc.edu.cn

but instead enters a dilute quantum droplet state stabilized by quantum fluctuations. Some experiments have demonstrated the stabilization of quantum droplets in the weakly interacting Bose-Bose mixture [9–11]. This provides a direct manifestation of effects beyond mean-field theory and has rekindled interest in exploring novel ground-state properties of these dilute, weakly interacting systems [12–15].

On the other hand, in recent years, the study of the physical properties of bubble-shaped Bose-Einstein condensates (BECs) has also received increasing attention. Unlike the situation in free space, bubble-shaped BECs, as the simplest boundaryless closed systems, have a unique advantage in exploring the effects of spatial curvature on the phase of ultracold gases due to their curved geometric structure and the isotropic nature in all spatial directions. Theoretically, extensive studies and various intriguing phenomena have been considered and predicted in such novel systems, including the Haldane spherical surface with a synthetic magnetic monopole [16–18], unique collective modes [19–21], self-interference patterns [19], and some interesting thermodynamic behaviors [22–24]. Additionally, closed-spherical-shell BECs can form stable vortex-antivortex pairs [25]. Further studies have investigated the Berezinskii-Kosterlitz-Thouless transition of spherical-shell BECs in the thin-shell limit, revealing the connection between BECs with curved geometry and superfluidity [22].

Experimentally, although the proposal for a bubble-shaped BEC involving rf-dressed magnetic traps with a nontrivial topology has been made by Zobay and Garraway in [26], the physical implementation in real systems has been achieved only recently due to the influence of the surface's gravitational field. In [27] Morizot *et al.* successfully confined ultracold atomic clouds on a spherical shell in experiments based on the theoretical framework proposed in Refs. [26,28]. However, due to the influence of gravity, ultracold atoms remained trapped near the bottom of an ellipsoidal surface, making it challenging to achieve a fully closed spherical shell. In [29] Carollo *et al.* observed ultracold atomic bubbles in orbital microgravity, where significant cooling associated with expansion has been demonstrated. Subsequently, by compensating for gravitational effects using inhomogeneous rf coupling, Guo *et al.* successfully created a closed spherical shell using a rf-dressed magnetic trap potential [30]. Meanwhile, Jia *et al.* also have successfully prepared a closed-shell BEC using a distinct method that relies on optically trapped double-species BECs of ^{87}Rb and ^{23}Na atoms in the immiscible phase under earth's gravity [31]. These experimental advancements thus provide a solid foundation for exploring novel physics due to interactions and curved geometries in spherical cold atoms, particularly the exotic states induced by quantum fluctuations.

In this paper we investigate the stability of binary-component Bose atoms in a spherical system and explore the existence of quantum droplets under the LHY correction induced by quantum fluctuations. We analytically calculate the ground-state energy density of a spherical two-dimensional weak-interaction Bose-Bose mixture under the Bogoliubov approximation and analyze the stability of the spherical Bose-Bose mixture. For weak interspecies attractive ($g_{12} < 0$) and intraspecies repulsive interactions ($\{g_{11}, g_{22}\} > 0$), in particu-

lar when $g_{11}g_{22} \simeq g_{12}^2$ where the mean-field interaction almost vanishes, we find that the energy per particle has a minimum value at finite density in the presence of the LHY correction. This means that the mixture that would collapse according to mean-field theory forms a quantum droplet stabilized by quantum fluctuations. To confirm the above analysis, we also numerically solve the extended Gross-Pitaevskii equation by incorporating both bubble traps and the additional energy due to quantum fluctuations. The results indicate that the formation of droplet states depends closely on the total particle numbers of the system due to the finite-size effect of the thin-spherical-shell traps. We find that the ratio of particle-number densities between the two bosonic species can drive the system's transition from a droplet state to a uniformly distributed spherical condensate, which is also qualitatively consistent with our estimation.

The structure of our paper is as follows. In Sec. II we analytically calculate the energy of a single-component spherical Bose gas using Bogoliubov theory. This calculation is then extended to the case of a spherical weakly interacting Bose-Bose mixture in Sec. III. In Sec. IV we theoretically explored the existence of droplet states on a two-dimensional sphere and the relationship between the equilibrium density and the system parameters. In Sec. V we numerically solve the extended Gross-Pitaevskii equation that includes both the spherical bubble potential and energy corrections due to quantum fluctuation. A summary is presented in Sec. VI.

II. ENERGY OF A SPHERICAL BOSE GAS

We start by considering the quantum fluctuations of a single-component Bose gas subject to a spherical-surface trap potential. The Hamiltonian of the system can be written as

$$\hat{H} = \int d\vec{r} \hat{\psi}^\dagger \left(-\frac{\hbar^2}{2m_0} \nabla^2 + \frac{g}{2} \hat{\psi}^\dagger \hat{\psi} \right) \hat{\psi}, \quad (3)$$

where

$$\begin{aligned} \nabla^2 &= \frac{1}{R^2 \sin \theta} \frac{\partial}{\partial \theta} \left(\sin \theta \frac{\partial}{\partial \theta} \right) + \frac{1}{R^2 \sin^2 \theta} \frac{\partial^2}{\partial \varphi^2}, \\ \hat{\psi} &= \sum_{lm} \frac{C_{l,m}}{R} Y_{l,m}(\theta, \varphi). \end{aligned} \quad (4)$$

Here m_0 and $\hat{\psi}$ are the mass and field operator of the boson, respectively; g is the strength of contact interaction; R is the radius of the surface trap; $Y_{l,m}(\theta, \varphi)$ is the spherical harmonic function; and $C_{l,m}$ is the bosonic annihilation operator corresponding to the angular momentum quantum numbers (l, m) . The total particle number \hat{N} of the system can be written as

$$\int d\vec{r} \hat{\psi}^\dagger \hat{\psi} = \sum_{l,m} C_{l,m}^\dagger C_{l,m} = \hat{N}. \quad (5)$$

In the case of low temperature and large N , these bosons condense to the ground state to form a BEC, i.e., $N \approx N_0$, where N_0 is the number of atoms in the BEC and N is the total number of atoms. Therefore, we can use the substitution $C_{00} \rightarrow \sqrt{N_0}$ and expand Eq. (3) to the bilinear terms of the operators $C_{l,m}^\dagger$ and $C_{l,m}$ ($l \neq 0$), which leads to the quadratic

Hamiltonian

$$\hat{H} = \frac{gN^2}{2S} + \sum'_{lm} [\varepsilon l(l+1) + gn] C_{lm}^\dagger C_{lm} + \frac{gn}{2} \sum'_{lm} (-1)^m (C_{lm} C_{l-m} + C_{lm}^\dagger C_{l-m}^\dagger), \quad (6)$$

where $\varepsilon = \hbar^2/2m_0 R^2$ and $S = 4\pi R^2$, \sum'_{lm} refers to the sum over all $l \neq 0$, and $n = N/S$ is the atomic number density. To obtain the excitation of the system, we introduce the Bogoliubov transformation as

$$\begin{aligned} C_{lm} &= u_{lm} \alpha_{lm} - v_{lm} \alpha_{l-m}^\dagger, \\ C_{lm}^\dagger &= u_{lm}^* \alpha_{lm}^\dagger - v_{lm}^* \alpha_{l-m}, \end{aligned} \quad (7)$$

with the constraint $|u_{lm}|^2 - |v_{lm}|^2 = 1$. Applying the standard Bogoliubov theory (see, for example, Ref. [32]), we can diagonalize Eq. (6) as

$$\hat{H} = \frac{gN^2}{2S} + \sum'_{l,m} E_l \alpha_{lm}^\dagger \alpha_{lm} + \frac{1}{2} \sum'_{l,m} (E_l - \epsilon_l - gn), \quad (8)$$

where the Bogoliubov excitation spectrum reads

$$E_l = \sqrt{\epsilon_l(\epsilon_l + 2gn)}, \quad (9)$$

with $\epsilon_l = \varepsilon l(l+1)$. Therefore, the ground-state energy can then be written as

$$E = \frac{gN^2}{2S} + \frac{1}{2} \sum_{l=1}^{l_c} (2l+1)(E_l - \epsilon_l - gn), \quad (10)$$

with the cutoff $l_c \gg 1$.

In Eq. (10) it can be seen that the first term is the dominant interaction energy which clearly represents the mean-field effect, while the second term originates from quantum fluctuations and serves as a higher-order correction. Combining Eqs. (8) and (10), it is evident that these higher-order corrections can be attributed to the vacuum zero-point energy of the Bogoliubov quasiparticle, indicating its quantum nature. If we define $\omega(l) = (2l+1)(E_l - \epsilon_l - gn)$ and apply the Euler-Maclaurin formula to the second order, we have

$$\sum_{l=1}^{l_c} \omega(l) \simeq \int_1^{l_c} \omega(l) dl - \frac{1}{2} \sum_{l=1}^{l_c} \frac{d\omega}{dl} - \frac{1}{6} \sum_{l=1}^{l_c} \frac{d^2\omega}{dl^2}. \quad (11)$$

The ground-state energy density can then be estimated as

$$\begin{aligned} \frac{E}{4\pi R^2} &= \frac{gn^2}{2} - \frac{m_0 g^2 n^2}{8\pi \hbar^2} \ln \frac{\hbar^2 l_c (l_c + 1)}{m_0 (E_1 + \epsilon_1 + gn) R^2 e^{1/2}} \\ &+ \frac{m_0 E_1}{8\pi \hbar^2} (E_1 - \epsilon_1 - gn) - \frac{C_1 gn}{4\pi R^2}, \end{aligned} \quad (12)$$

where $\epsilon_1 = 2\varepsilon$, $E_1 = \sqrt{\epsilon_1(\epsilon_1 + 2gn)}$, and $C_1 \simeq 0.62$ is obtained from the numerical fit [33] of the summation correction term in Eq. (11).

To eliminate the dependence of energy density on the cutoff l_c , we introduce the renormalization condition in Ref. [33], which can be rewritten in our case as

$$\frac{1}{g} = \frac{m_0}{4\pi \hbar^2} \ln \frac{4R^2}{l_c(l_c + 1)a^2 e^{2\gamma}}. \quad (13)$$

Finally, we obtain the ground-state energy density of the system as

$$\begin{aligned} \frac{E}{4\pi R^2} &= gn^2 - \frac{m_0 g^2 n^2}{8\pi \hbar^2} \ln \left(\frac{4\hbar^2}{m_0 (E_1 + \epsilon_1 + gn) a^2 e^{2\gamma + 0.5}} \right) \\ &+ \frac{m_0 E_1}{8\pi \hbar^2} (E_1 - \epsilon_1 - gn) - \frac{C_1 gn}{4\pi R^2}, \end{aligned} \quad (14)$$

where γ is the Euler-Mascheroni constant and a is the spherical s -wave scattering length. In particular, when $R \rightarrow \infty$, we have $E_1 \simeq 0$ and $\epsilon_1 \simeq 0$. Therefore, Eq. (14) reduces to the ground-state energy density of a weakly interacting Bose gas in the two-dimensional plane case as $E_{2D} \simeq gn^2 - c_1 g^2 n^2 [\ln(c_2/gn)]$ [2,3,34,35], where c_1 and c_2 are quantities that are independent of n . It is evident that this expression includes contributions from both the mean-field interaction and the dominant corrections beyond mean-field terms.

Additionally, for a three-dimensional homogeneous Bose gas, it is well known that the long-wavelength excitations are sound waves, which also means that its low-energy excitation is gapless [8,36]. However, in a spherical-surface system, the single-particle eigenstates are discrete and have good quantum numbers (l, m) defined by the angular momentum operators (L^2, L_z) . Thus, the Bogoliubov excitation spectra of the spherical system are also discrete and the excitation is gapped. We note that higher-order quantum fluctuation effects can also be taken into account by considering the cubic or higher terms of the operators C_{lm}^\dagger and C_{lm} ($l \neq 0$). This allows for further exploration of the interaction between quasiparticles in the spherical two-dimensional Bose gas, which may lead to the corresponding Beliaev damping on the spherical-surface system.

III. BOSE-BOSE MIXTURE ON A SPHERICAL SURFACE

The discussion in Sec. II can also be generalized to the case of a two-component BEC on the spherical surface. Specifically, the Hamiltonian for the Bose-Bose mixture on the surface of a sphere can be written as $\hat{H} = \int d\mathbf{r} \hat{h}$, with

$$\hat{h} = \sum_{i=1,2} \hat{\psi}_i^\dagger \left(-\frac{\hbar^2 \nabla^2}{2m_i} \right) \hat{\psi}_i + \sum_{ij} \frac{g_{ij}}{2} \hat{\psi}_i^\dagger \hat{\psi}_j^\dagger \hat{\psi}_j \hat{\psi}_i \hat{\psi}_i. \quad (15)$$

Here m_i and $\hat{\psi}_i$ denote the mass and field operators of bosonic species i , respectively. The intra- and interspecies coupling constants g_{ii} and g_{12} , respectively, are related to the corresponding s -wave scattering lengths, which can be tuned by Feshbach resonance. We then expand the field operators $\hat{\psi}_1(\theta, \varphi)$ and $\hat{\psi}_2(\theta, \varphi)$ in terms of spherical harmonics as

$$\begin{aligned} \hat{\psi}_1(\theta, \varphi) &= \sum_{lm} \frac{\hat{a}_{l,m}}{R} Y_{l,m}(\theta, \varphi), \\ \hat{\psi}_2(\theta, \varphi) &= \sum_{lm} \frac{\hat{b}_{l,m}}{R} Y_{l,m}(\theta, \varphi), \end{aligned} \quad (16)$$

where $\hat{a}_{l,m}$ and $\hat{b}_{l,m}$ are the annihilation operators of the two species with angular momentum quantum numbers (l, m) , respectively. The total particle numbers \hat{N}_1 and \hat{N}_2 of the two

species can be rewritten as

$$\int d\vec{r} \hat{\psi}_1^\dagger(\theta, \varphi) \hat{\psi}_1(\theta, \varphi) = \sum_{l,m} a_{lm}^\dagger a_{lm} = \hat{N}_1,$$

$$\int d\vec{r} \hat{\psi}_2^\dagger(\theta, \varphi) \hat{\psi}_2(\theta, \varphi) = \sum_{l',m'} b_{l'm'}^\dagger b_{l'm'} = \hat{N}_2. \quad (17)$$

Next, following the treatment of a single-component Bose gas in Sec. II, we consider the fluctuations beyond the mean-field effect based on the standard Bogoliubov theory. After expanding the Hamiltonian of the system in terms of the operators a_{lm}^\dagger , a_{lm} , b_{lm}^\dagger , and b_{lm} ($l \neq 0$), we obtain the quadratic Hamiltonian as

$$\hat{H} = \sum_{ij} \frac{g_{ij} N_i N_j}{2S} + h_1 + h_2 + h_{12}. \quad (18)$$

Here h_i represents the effective interactions within a single component and h_{12} denotes the coupling between the two bosonic excitations, whose explicit forms read

$$h_1 = \sum'_{lm} [\varepsilon_l l(l+1) + g_{11} n_1] a_{lm}^\dagger a_{lm} + \frac{g_{11} n_1}{2} \sum'_{lm} (-1)^m (a_{lm} a_{l-m} + a_{lm}^\dagger a_{l-m}^\dagger),$$

$$h_2 = \sum'_{lm} [\varepsilon_l l(l+1) + g_{22} n_2] b_{lm}^\dagger b_{lm} + \frac{g_{22} n_2}{2} \sum'_{lm} (-1)^m (b_{lm} b_{l-m} + b_{lm}^\dagger b_{l-m}^\dagger),$$

$$h_{12} = g_{12} \sqrt{n_1 n_2} \sum'_{lm} [(-1)^m a_{lm} b_{l-m} + (-1)^m a_{lm}^\dagger b_{l-m}^\dagger + b_{lm}^\dagger a_{lm} + a_{lm}^\dagger b_{lm}]. \quad (19)$$

Here $\varepsilon_i = \hbar^2/2m_i R^2$ and $n_i = N_i/S$ is the particle-number density of boson species i . The notation \sum'_{lm} refers to the sum excluding $l = 0$. To facilitate the subsequent discussion, we consider the case of two equal-mass bosonic species with $m_1 = m_2 = M$. After introducing the Bogoliubov transformations

$$a_{lm} = u_{lm} \alpha_{lm} - v_{lm} \alpha_{l-m}^\dagger + x_{lm} \beta_{lm} - y_{lm} \beta_{l-m}^\dagger,$$

$$b_{lm} = x_{lm} \alpha_{lm} - y_{lm} \alpha_{l-m}^\dagger + u_{lm} \beta_{lm} - v_{lm} \beta_{l-m}^\dagger \quad (20)$$

and applying the standard Bogoliubov theory [32], we can diagonalize Eq. (18) and obtain the ground-state energy density as

$$E = \frac{1}{2} \sum_{i,j} g_{ij} n_i n_j + \frac{1}{8\pi R^2} \sum'_{l,m} [E_+(l, m) + E_-(l, m) - 2\varepsilon_l(l+1) - g_{11} n_1 - g_{22} n_2] \quad (i, j = 1, 2), \quad (21)$$

where

$$E_\pm(l, m) = \sqrt{\varepsilon_l(l+1)[\varepsilon_l(l+1) + 2c_\pm^2]} \quad (22)$$

are the excitation energies of Bogoliubov modes with

$$c_\pm^2 = \frac{g_{11} n_1 + g_{22} n_2 \pm \sqrt{(g_{11} n_1 - g_{22} n_2)^2 + 4g_{12}^2 n_1 n_2}}{2} \quad (23)$$

and $\varepsilon = \hbar^2/2MR^2$. It is easy to verify that despite the mean-field term $E_{\text{MF}} = \frac{1}{2} \sum_{i,j} g_{ij} n_i n_j$, the second term of Eq. (21) represents the LHY correction E_{LHY} caused by quantum fluctuations.

IV. LHY CORRECTION OF BOSE-BOSE MIXTURE ON THE SURFACE OF A SPHERE

Although the LHY correction E_{LHY} has been theoretically predicted for more than 60 years [8], for dilute gases, the correction energy is relatively small compared to the mean-field interaction, making its effect generally difficult to observe experimentally. On the other hand, increasing the strength of interactions through Feshbach resonance may lead to the presence of other more significant higher-order effects of the system, which is also unfavorable for detecting the effects. However, for the Bose-Bose mixture, it has been illustrated in [7,12] that, under certain special interaction parameters, i.e., when the dominant mean-field term is very small and negligible, weakly interacting systems may also exhibit significant quantum fluctuation effects.

Specifically, we consider the typical case with weak intraspecies repulsive and interspecies attractive interactions between the two components, i.e., $(g_{11}, g_{22}) > 0$, and $g_{12} < 0$ with

$$\frac{1}{a_{12}} \ll \{\sqrt{n_1}, \sqrt{n_2}\} \ll \left\{ \frac{1}{a_{11}}, \frac{1}{a_{22}} \right\}, \quad (24)$$

where a_{11} , a_{22} , and a_{12} are the intraspecies and interspecies scattering lengths of components 1 and 2, respectively. In particular, when $g_{12}^2 = g_{11} g_{22}$, we can rewrite the mean-field term of the ground-state energy density (21) as

$$E_{\text{MF}} = \frac{1}{2} (\sqrt{g_{11}} n_1 - \sqrt{g_{22}} n_2)^2. \quad (25)$$

If we lock the density ratio of the two components to $n_1/n_2 = \sqrt{g_{22}/g_{11}}$, then E_{MF} becomes negligible and the nonzero correction term E_{LHY} caused by quantum fluctuations will dominate. To obtain the explicit form of E_{LHY} , we substitute $g_{12}^2 = g_{11} g_{22}$ into Eq. (21) as

$$E_{\text{LHY}} = \frac{1}{8\pi R^2} \sum'_{l,m} \{ \sqrt{\varepsilon_l [\varepsilon_l + 2(g_{11} n_1 + g_{22} n_2)]} - \varepsilon_l - g_{11} n_1 - g_{22} n_2 \}, \quad (26)$$

with $\varepsilon_l = \varepsilon_l(l+1)$. Similarly, by introducing the cutoff $l_c \gg 1$, we can calculate the summation in Eq. (26) and rewrite E_{LHY} as

$$E_{\text{LHY}} = \frac{M \mu_{12}^2}{8\pi \hbar^2} \ln \left(\frac{M(E_1 + 2\varepsilon + \mu_{12}) R^2 e^{1/2}}{\hbar^2 l_c (l_c + 1)} \right) + \frac{M E_1}{8\pi \hbar^2} (E_1 - 2\varepsilon - \mu_{12}) - \frac{C_1 \mu_{12}}{4\pi R^2}, \quad (27)$$

where $\mu_{12} = g_{11} n_1 + g_{22} n_2$, $C_1 \simeq 0.62$, and $E_1 = \sqrt{2\varepsilon [2\varepsilon + 2(g_{11} n_1 + g_{22} n_2)]}$. It is evident that, when either of the particle-number densities n_i is zero, Eq. (27) reduces to the single-component case described in Sec. II, which validates our derivation. Additionally, it is worth noting that in the two-dimensional case, the coupling parameters g_{11} , g_{22} , and g_{12} are not only related to their respective scattering

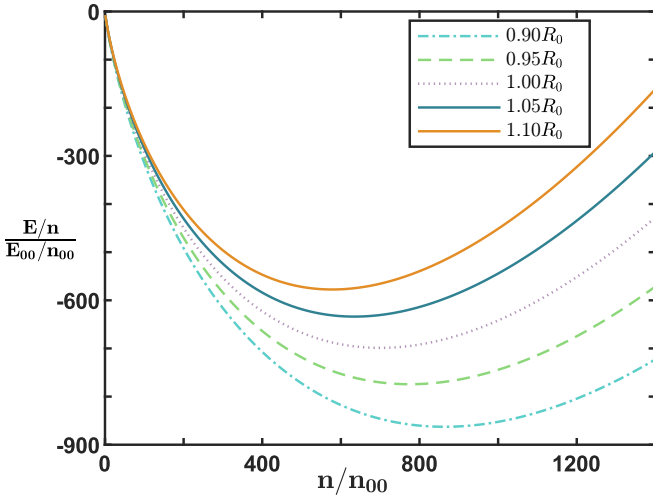


FIG. 1. Energy per particle of the symmetric Bose-Bose mixture, E/n , as a function of the particle-number density n , for different sphere radii R . We normalize the vertical axis units to $E_{00}/n_{00} = g/4\pi R_0^2$ and the horizontal axis units to $n_{00} = \hbar^2/2MR_0^2$. Clearly, the energy per particle has a minimum value with respect to the particle-number density n . As the sphere radius R increases, the equilibrium density gradually decreases.

lengths, but also dependent on the cutoff l_c . This relationship ensures that the ground-state energy density E of the system can be independent of the cutoff l_c , i.e., $\partial E/\partial l_c = 0$ [12,15].

By applying the renormalized relation on the surface of the sphere shown in (13), we can rewrite the LHY correction term E_{LHY} as the total energy density for the symmetric Bose-Bose mixture as

$$E = \frac{Mg^2 n^2}{2\pi\hbar^2} \ln \left(\frac{M(E_1 + 2\varepsilon + 2gn)aa_{12}e^{2\gamma+1/2}}{4\hbar^2} \right) + \frac{ME_1}{8\pi\hbar^2}(E_1 - 2\varepsilon - 2gn) - \frac{C_1 gn}{2\pi R^2}, \quad (28)$$

where the mean-field term E_{MF} disappears as we have set $g_{11} = g_{22} = g$, $a_{11} = a_{22} = a$, and $n_1 = n_2 = n$. Therefore, the ground state of the condensates is completely determined by the higher-order correction term E_{LHY} caused by quantum fluctuations. Notably, Eq. (28) is also consistent with the result for the two-dimensional plane case when $R \rightarrow \infty$ [12].

To illustrate that quantum fluctuation is crucial for the stability of this weak-interaction system, in Fig. 1 we plot the dependence of the mean energy density per particle E/n as described by Eq. (28) on particle-number density n using typical experimental parameters $aa_{12}/8R^2 = 5 \times 10^{-5}$ [33,37]. Clearly, the energy per particle E/n reaches a minimum value with respect to n . The equilibrium density n_0 can then be theoretically determined by the relation $\partial(E/n)/\partial n = 0$. Additionally, in the dilute limit, Eq. (28) shows that as $n \rightarrow 0$, $E/n \propto n(gn/\varepsilon - 6.86)$, indicating that E/n monotonically decreases with n . Conversely, when $n \rightarrow \infty$, we have $E/n \propto gn[\ln(gn/\varepsilon) - 7.55]/\varepsilon - \sqrt{2gn/\varepsilon}$, which means that E/n monotonically increases with n in this opposite case. Therefore, there must exist a certain n_0 such that the energy reaches a minimum.

The presence of the equilibrium density n_0 can lead to typical dynamical behavior of quantum droplets due to the finite-size feature of the spherical surface. Specifically, assume the Bose-Bose mixture uniformly occupies the entire sphere. If the initial particle-number density n is less than n_0 , the system will evolve to minimize its total energy, causing the density to approach the equilibrium value n_0 . Consequently, the Bose-Bose mixture will not occupy the entire sphere at equilibrium, and quantum droplets with self-bound properties may form on the sphere. This provides a direct manifestation of quantum fluctuations beyond mean-field effects. Conversely, if the initial local particle-number density $n > n_0$, the system tends to decrease the density n to minimize the total mean energy density E/n . However, due to the finite-size effects associated with the spherical geometry, even after reaching equilibrium, the Bose-Bose mixture is distributed over the entire sphere and does not form a self-bound droplet state. This is very different from the case of a free symmetric Bose-Bose mixture [12], where, regardless of the initial density, the density n of the system will approach the equilibrium density n_0 as the total energy of the system tends to its minimum. Therefore, a free Bose-Bose mixture always forms self-bound droplets at equilibrium.

Next we consider the symmetric Bose-Bose mixture with $g_{12}/g = \lambda$. Following the previous treatment, we obtain the ground-state energy density

$$E = E_{\text{MF}} + E_{\text{LHY}}, \quad (29)$$

where

$$E_{\text{MF}} = (1 + \lambda)gn^2, \\ E_{\text{LHY}} = \frac{Mg^2 n^2 (1 - \lambda)^2}{8\pi\hbar^2} \ln \left(\frac{E_1 + 2\varepsilon + (1 - \lambda)gn}{\hbar^2 l_c (l_c + 1) (MR^2 e^{1/2})^{-1}} \right) + \frac{ME_1}{8\pi\hbar^2} [E_1 - 2\varepsilon - (1 - \lambda)gn] - \frac{C_1 (1 - \lambda)gn}{4\pi R^2} + \frac{Mg^2 n^2 (1 + \lambda)^2}{8\pi\hbar^2} \ln \left(\frac{E_2 + 2\varepsilon + (1 + \lambda)gn}{\hbar^2 l_c (l_c + 1) (MR^2 e^{1/2})^{-1}} \right) + \frac{ME_2}{8\pi\hbar^2} [E_2 - 2\varepsilon - (1 + \lambda)gn] - \frac{C_2 (1 + \lambda)gn}{4\pi R^2}, \quad (30)$$

with $E_{k=1,2} = \sqrt{2\varepsilon \{2\varepsilon + 2[1 + (-1)^k \lambda]gn\}}$ and $C_1 = C_2 \simeq 0.62$ parameters obtained through numerical fitting. It is evident that when $\lambda = -1$, Eq. (29) reduces to Eq. (27). If $\lambda \neq -1$, the mean-field term E_{MF} will not be zero. From Eq. (30) we find that $E_{\text{MF}}/n \propto n$, indicating that this term does not tend to provide a single-particle energy minimum. Additionally, when λ deviates slightly from -1 , within a certain range of particle-number density, the correction term E_{LHY} should still be comparable to the mean-field term E_{MF} . Thus, the energy per particle will still exhibit a minimum value. However, when λ deviates significantly from -1 , within the typical experimental parameter range [33,37], the energy per particle may no longer exhibit a minimum value, as the mean-field term E_{MF} becomes the dominant term in the ground-state energy density.

By applying the renormalized relation on the surface of the sphere as shown in (13), the ground-state energy density (29)

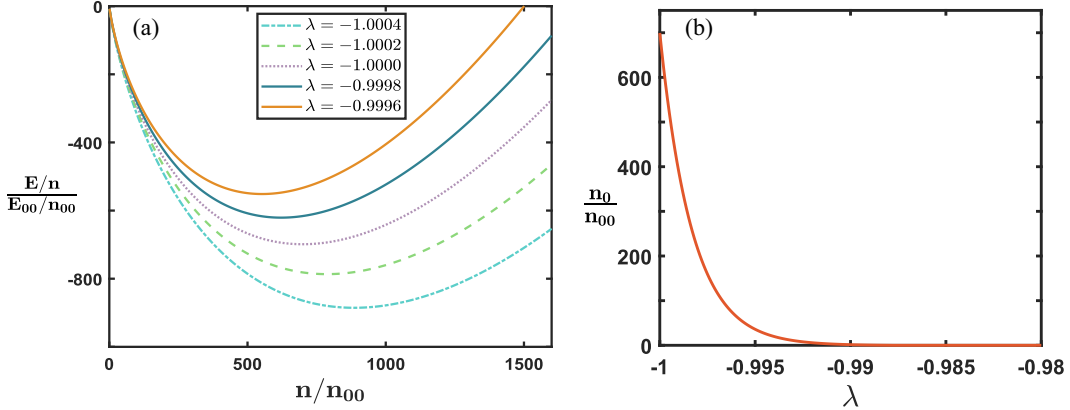


FIG. 2. (a) Dependence of the energy per particle E/n on the particle-number density n for different values of λ . The units of the vertical axis are adjusted to $E_{00}/n_{00} = g/4\pi R^2$ and the units of the horizontal axis are adjusted to $n_{00} = \varepsilon/g$. Clearly, when λ deviates slightly from -1 , the energy per particle still exhibits a minimum with respect to the particle-number density. (b) Variation of the possible equilibrium density n_0 of a symmetric Bose-Bose mixture with λ . The units of the vertical axis are adjusted to $n_{00} = \varepsilon/g$. As λ gradually increases, the equilibrium density n_0 decreases.

can be rewritten as

$$\begin{aligned} E = & 2(1 + \lambda)gn^2 + \frac{M\lambda^2g^2n^2}{4\pi\hbar^2} \ln \frac{a_{12}^2}{a^2} \\ & + \frac{Mg^2n^2(1 - \lambda)^2}{8\pi\hbar^2} \ln \left(\frac{E_1 + 2\varepsilon + (1 - \lambda)gn}{4\hbar^2(Ma^2e^{2\gamma+1/2})^{-1}} \right) \\ & + \frac{ME_1}{8\pi\hbar^2}[E_1 - 2\varepsilon - (1 - \lambda)gn] - \frac{C_1(1 - \lambda)gn}{4\pi R^2} \\ & + \frac{Mg^2n^2(1 + \lambda)^2}{8\pi\hbar^2} \ln \left(\frac{E_2 + 2\varepsilon + (1 + \lambda)gn}{4\hbar^2(Ma^2e^{2\gamma+1/2})^{-1}} \right) \\ & + \frac{ME_2}{8\pi\hbar^2}[E_2 - 2\varepsilon - (1 + \lambda)gn] - \frac{C_2(1 + \lambda)gn}{4\pi R^2}. \quad (31) \end{aligned}$$

Figure 2(a) shows the dependence of the energy per particle E/n as described by Eq. (31) on the particle-number density n for different values of λ . Here we set $2\pi\hbar^2/Mg = 300$, $a_{12}/a = 1 \times 10^4$, and $a^2/8R^2 = 5 \times 10^{-9}$. We also numerically calculated the possible equilibrium density n_0 as λ varies, as shown in Fig. 2(b). It is evident that as λ increases, the equilibrium density n_0 decreases. This result is consistent with our previous analysis. Additionally, it can be observed from the expression (31) that when λ is much smaller than -1 , the excitation energy E_2 of the Bogoliubov mode can be complex. Therefore, the ground-state energy density of the system takes an imaginary part, indicating the presence of instability in the system. The stabilization of the system due to quantum fluctuation works only when the interspecies attractive interaction cannot be excessively strong.

Finally, when the densities of the two components are unequal and satisfy $n_1 = n$ and $n_2 = \eta n$, the ground-state energy density can then be expressed as in Eq. (29) where

$$\begin{aligned} E_{\text{MF}} &= \frac{1}{2}gn^2(1 - \eta)^2, \\ E_{\text{LHY}} &= \frac{Mg^2n^2(1 + \eta)^2}{8\pi\hbar^2} \ln \left(\frac{E_1 + 2\varepsilon + gn(1 + \eta)}{\hbar^2l_c(l_c + 1)(MR^2e^{1/2})^{-1}} \right) \\ &+ \frac{ME_1}{8\pi\hbar^2}[E_1 - 2\varepsilon - gn(1 + \eta)] - \frac{C_1gn(1 + \eta)}{4\pi R^2}, \quad (32) \end{aligned}$$

with $C_1 \simeq 0.62$ and $E_1 = \sqrt{2\varepsilon[2\varepsilon + 2gn(1 + \eta)]}$. It is easy to verify that for a symmetric Bose-Bose mixture with $\eta = 1$, Eq. (29) reduces to Eq. (27) and the mean-field term E_{MF} disappears. However, when η deviates from 1, the ground-state energy density E will be dominated by the mean-field term E_{MF} , which is minimized only when $n = 0$ and does not favor an equilibrium state with the finite particle-number density n_0 . Nevertheless, around $\eta \sim 1$, within a certain range of particle-number density, the correction term E_{LHY} due to quantum fluctuations should be comparable to the mean-field term [33,37]. Therefore, in this case, the energy per particle E/n still has a minimum value with respect to the particle-number density n .

By applying the renormalized relation on the surface of the sphere as shown in (13), the ground-state energy density (29) can be rewritten as

$$\begin{aligned} E = & gn^2(1 - \eta)^2 + \frac{M\eta g^2n^2}{4\pi\hbar^2} \ln \frac{a_{12}^2}{a^2} \\ & + \frac{Mg^2n^2(1 + \eta)^2}{8\pi\hbar^2} \ln \left(\frac{E_1 + 2\varepsilon + (1 + \eta)gn}{4\hbar^2(Ma^2e^{2\gamma+1/2})^{-1}} \right) \\ & + \frac{ME_1}{8\pi\hbar^2}[E_1 - 2\varepsilon - gn(1 + \eta)] - \frac{C_1gn(1 + \eta)}{4\pi R^2}. \quad (33) \end{aligned}$$

In Fig. 3(a) we plot the relationship between the energy per particle E/n and the particle-number density n for different values of η , based on the parameters corresponding to Fig. 2. We can observe that when η deviates slightly from 1, the energy per particle E/n still has a minimum value with respect to the particle-number density n . However, as η gradually deviates further from 1, the minimum point of the energy per particle, corresponding to the equilibrium density n_0 , becomes smaller and its corresponding minimum value becomes larger, indicating a decreased influence of the quantum fluctuation effects on the system. To further analyze this, we illustrate the variation of the possible equilibrium density n_0 as η gradually deviates from 1 in Fig. 3(b). It is evident that as η deviates further from 1, the equilibrium density decreases to zeros almost exponentially with the parameter $\eta - 1$, which confirms our previous discussion.

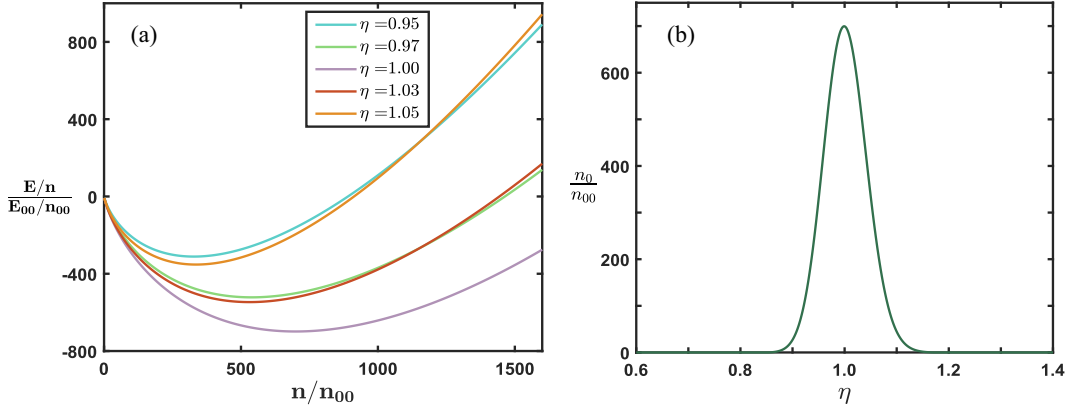


FIG. 3. (a) Values of the energy per particle E/n as a function of the particle-number density n , for different values of η , as described by Eq. (33). Here we adjust the units of the vertical axis to $E_{00}/n_{00} = g/4\pi R^2$ and the units of the horizontal axis to $n_{00} = \varepsilon/g$. It is evident that when the value of η deviates slightly from 1, the energy per particle still has a minimum value with respect to the particle-number density. (b) Variation of the possible equilibrium density as η deviates gradually from 1. Here we adjust the units of the vertical axis to $n_{00} = \varepsilon/g$. It can be intuitively observed that as η deviates from 1, the equilibrium density gradually decreases.

V. NUMERICAL DENSITY DISTRIBUTION OF TWO-COMPONENT BECs IN A SPHERICAL-SHELL TRAP

Although a strict two-dimensional spherical BEC system is still difficult to achieve, spherical-shell-shaped constrained systems for ultracold quantum gases can currently be constructed in both space-based and ground-based environments [29–31]. In this section we numerically solve the coupled extended Gross-Pitaevskii equation to obtain the ground-state density distribution of a two-component BEC in the spherical-shell trap by taking into account the LHY corrections, which also partly confirms our previous discussion.

We start by considering the Hamiltonian of the Bose-Bose mixture in three-dimensional free space given by $\hat{H}_0 = \int d\mathbf{r} \hat{h}_0$, where

$$\hat{h}_0 = \sum_{i=1,2} \psi_i^\dagger \left(-\frac{\hbar^2 \nabla^2}{2m_i} \right) \psi_i(\mathbf{r}) + \sum_{ij} \frac{g_{ij}}{2} \psi_i^\dagger \psi_j^\dagger \psi_j \psi_i, \quad (34)$$

$$\epsilon_{\text{LHY}} = \int \frac{d^3\mathbf{k}}{2(2\pi)^3} \left(\sum_{i=1}^2 (E_{i\mathbf{k}} - \epsilon_{i\mathbf{k}} - g_{ii}n_i) + \sum_{ij} \frac{mg_{ij}^2 n_i n_j}{\hbar^2 \mathbf{k}^2} \right) = \frac{8}{15\pi^2 \hbar^3} m^{3/2} (g_{11}n_1)^{5/2} f \left(\frac{g_{12}^2}{g_{11}g_{22}}, \frac{g_{22}n_2}{g_{11}n_1} \right). \quad (36)$$

Here $E_{i\mathbf{k}}$ is the Bogoliubov spectrum and $f > 0$ is a dimensionless quantity that reads

$$f(x, y) = \sum_{\pm} \frac{1}{4\sqrt{2}} (1 + y \pm \sqrt{(1 - y)^2 + 4xy})^{5/2}. \quad (37)$$

We stress that, formally, the LHY energy density correction becomes complex when $g_{12}^2 > g_{11}g_{22}$, i.e., it becomes ill-defined. Fortunately, it has been shown that the complexified energy density can be naturally eliminated through the introduction of bosonic pairing [14]. For our purpose, we assume that $|\delta g|$ is small compared to g_{11} (or g_{22}), that is, $g_{12}^2/g_{11}g_{22} \approx 1$ [7]. Following the analysis in Ref. [38], we

where m_i is the mass of the bosonic component i . For two equal-mass bosonic species ($m_1 = m_2 = m$), the interaction coupling constant between components i and j is $g_{ij} = 4\pi\hbar^2 a_{ij}/m$, where a_{ij} is the s -wave scattering length. Additionally, to illustrate the effect of LHY corrections, we consider the weak interspecies attractive and intraspecies repulsive interactions, namely, $g_{12} < 0$, $g_{11} > 0$, and $g_{22} > 0$, and require $\delta g = g_{12} + \sqrt{g_{11}g_{22}} < 0$. For a homogeneous system with uniform density n_i ($i = 1, 2$), the ground-state energy density under the mean field is given by

$$\epsilon_{\text{MF}} = \frac{1}{2} \sum_{i,j=1}^2 g_{ij} n_i n_j. \quad (35)$$

According to the standard Bogoliubov theory [8], the corresponding LHY energy density correction is

can rewrite ϵ_{LHY} as

$$\epsilon_{\text{LHY}} \simeq \frac{8m^{3/2}(g_{11}n_1)^{5/2}}{15\pi^2 \hbar^3} \left(1 + \frac{g_{22}n_2}{g_{11}n_1} \right)^{5/2}. \quad (38)$$

Therefore, the extended Gross-Pitaevskii equation can then be obtained as

$$i\hbar \frac{\partial \psi_i}{\partial t} = \left(-\frac{\hbar^2 \nabla^2}{2m} + V_i + \sum_{j=1}^2 g_{ij} |\psi_j|^2 + \frac{\partial \epsilon_{\text{LHY}}}{\partial n_i} \right) \psi_i, \quad (39)$$

where $n_i = |\psi_i|^2$ ($i = 1, 2$) is the particle-number density of component i . The external potential is given by $V_1 = V_2 = \frac{1}{2}m\omega^2(r - R)^2$. When the radius R is much larger than the characteristic length $l_T = \sqrt{\hbar/m\omega}$, the radial excitation energy is much greater than that of the transverse excitations, so

the radial wave function of the atom remains in the ground state. Thus, we can express the wave function as $\psi(\mathbf{r}) = \psi(\theta, \varphi)\phi_0(r)$, where $\phi_0(r)$ denotes the ground state of the harmonic oscillator. In this case, $\psi(\theta, \varphi)$ represents the effective two-dimensional wave function of the condensate on a spherical surface, with a corresponding two-dimensional atomic density n_s . In particular, when considering very strong harmonic confinement, i.e., $gn_s/l_T\hbar\omega \ll 1$ (we omit subscripts assuming that the coupling constants are of the same order of magnitude $\{g_{11}, g_{12}, g_{22}\} \sim g$), then following similar treatments as in Ref. [15], a perturbative approach allows us to rewrite the LHY contribution in the form obtained for the spherical two-dimensional system. The dimensionless Gross-Pitaevskii equations can then be rewritten as

$$i\frac{\partial\tilde{\phi}_i}{\partial\tilde{t}} = \left[-\frac{\nabla^2}{2} + \tilde{V}_i + \sum_{j=1}^2 \beta_{ij} |\tilde{\phi}_j|^2 + \delta_{ii} \left(|\tilde{\phi}_i|^2 + \frac{g_{jj}N_j}{g_{ii}N_i} |\tilde{\phi}_j|^2 \right)^{3/2} \right] \tilde{\phi}_i, \quad (40)$$

where $\psi_i = \sqrt{N_i}l_T^{-3/2}\tilde{\phi}_i$, $\tilde{t} = t\omega$, $\tilde{r} = r/l_T$, $\tilde{R} = R/l_T$, $\tilde{V}_i = (\tilde{r} - \tilde{R})^2/2$, $\beta_{ij} = g_{ij}N_j/\hbar\omega l_T^3$, and δ_{ii} is the contribution of quantum fluctuation that reads

$$\delta_{ii} \approx \frac{4m^{3/2}g_{ii}^{5/2}N_i^{3/2}}{3\pi^2\hbar^4\omega l_T^{9/2}}. \quad (41)$$

In order to obtain the ground state of the system under given parameters, we solved Eq. (40) using the imaginary-time method [39]. The ground-state properties of the system can be derived from the density and phase distributions of the condensates.

In Fig. 4(a) we numerically plot the dependence of the ground-state energy per particle E on the total particle number N for different g_{12} with fixed $\tilde{R} = 12$ and $g_{11}g_{22} = 1$. It is evident that the larger $|g_{12}|$ is, the stronger the interspecies attractive interaction becomes, resulting in a larger equilibrium particle-number density of the system. This is consistent with the physical behavior depicted in Fig. 2. Additionally, in the case of $g_{12} = -1.05$, three different initial particle-number densities are considered with $N = 0.66N_0$, $1.54N_0$, and $3.2N_0$, respectively, where the equilibrium particle-number density is obtained with $N_0 \simeq 3.0N_0$ for these typical parameter settings. The corresponding ground-state density profiles of the Bose-Bose mixture integrated along the radial direction \hat{r} are shown in Figs. 4(b)–4(d), respectively. It can be observed that when the average atomic density is lower than the equilibrium density with $N < N_0$, the condensates tend to cluster together in order to lower the total energy of the system, with the density of atoms within the condensates approximating the equilibrium density. As the number of particles increases, the condensate gradually expands and finally spreads across the entire surface of the sphere when the average density is greater than the equilibrium density. As the number of atoms is further increased, due to the finite size of the sphere, the atomic density of the condensates will increase and at the same time the average particle energy E will also increase gradually. Clearly, the behavior presented here is consistent with the physical picture analyzed in Sec. IV.

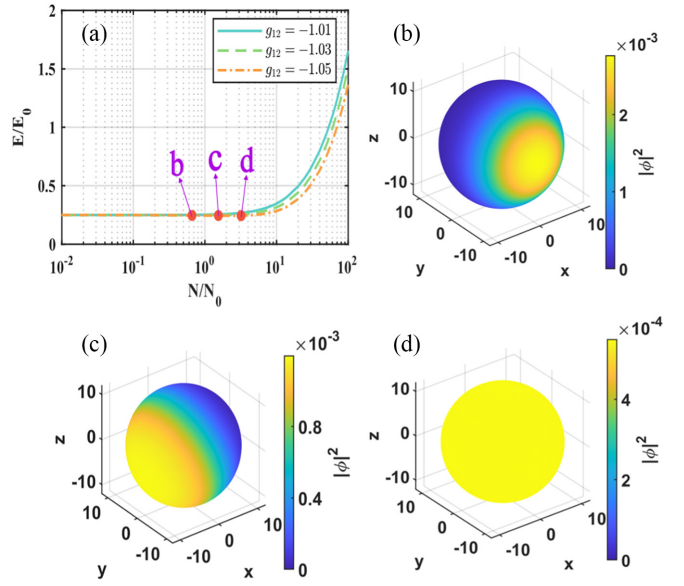


FIG. 4. (a) Dependence of the energy per particle E on the particle number N for different values of g_{12} . Clearly, the smaller the g_{12} , indicating a stronger interspecies attractive interaction, the larger the equilibrium particle-number density of the system. This behavior aligns with the physical observations presented in Fig. 2. Also shown are the ground-state density profiles of the Bose-Bose mixture integrated along the radial direction \hat{r} for the total particle numbers (b) $N = 0.66N_0$, (c) $N = 1.54N_0$, and (d) $N = 3.2N_0$ when $g_{12} = -1.05$ and $N_0 = 10^5$.

Moreover, we can also investigate the dependence of the ground-state profiles of the condensates on the radius of the spherical shell \tilde{R} . It is easy to verify that for small \tilde{R} , the atoms are distributed across the entire surface of the sphere, and the average atomic density will decrease for larger \tilde{R} as the surface area of the spherical shell also becomes larger. When the average density n is less than the critical equilibrium density, the condensate will cluster together to occupy a spherical cap, rather than being spread across the entire surface of the sphere. This phenomenon corresponds to the formation of droplet states. Physically, when the radius of the sphere is large, the system becomes more like a quasi-two-dimensional system rather than the usual three-dimensional system when $\tilde{R} \ll 1$. The formation of droplets also indicates that in lower dimensions, droplet states can be more stable and easier to form, which is consistent with existing conclusions. In Fig. 5 we numerically present the variation of the ground-state density profiles of the Bose-Bose mixture after integration along the radial direction \hat{r} with different spherical shells \tilde{R} , where all parameters, except for the spherical-shell radius \tilde{R} , remain consistent with those in Fig. 4(d). The numerical results are consistent with our expectations.

In the above discussion, we assumed that the numbers of particles in the two components are equal. We can also examine scenarios where the particle numbers of the two components are unequal, with the particle number of component 1 denoted by N_1 and that of component 2 is $N_2 = \eta N_1$. For the purpose of comparison, we also fix the intraspecies interactions for both components as $g_{11} = g_{22}$. During the calculations, we assume that the particle number of component

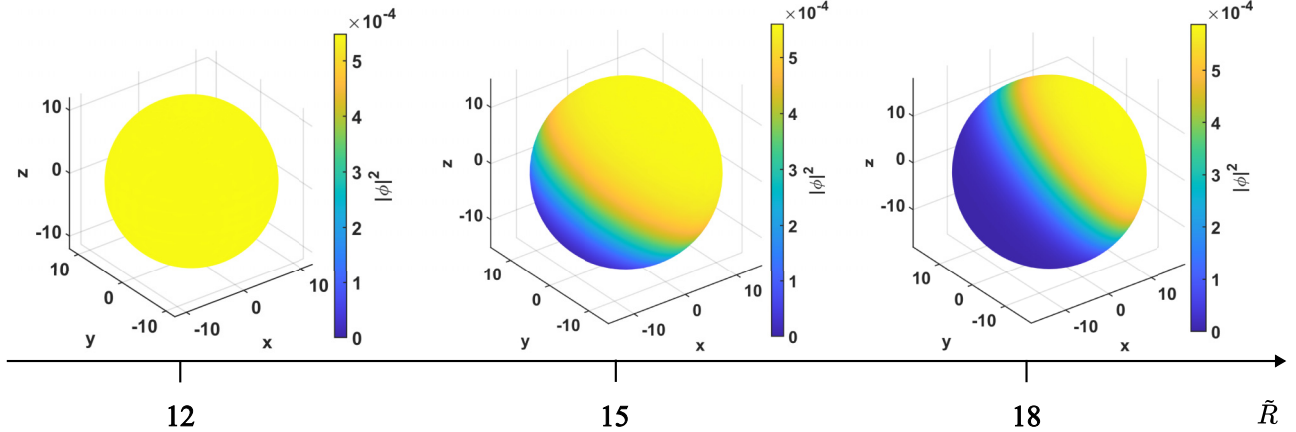


FIG. 5. Ground-state density profiles of the Bose-Bose mixture, integrated along the radial direction \hat{r} , for different radii of the spherical shell $\tilde{R} = 12, 15$, and 18 . The other parameters are $N = 3.2N_0$, $g_{12} = -1.05$, and $N_0 = 10^5$. It can be observed that the condensate will cluster together to occupy a spherical cap, rather than spreading uniformly across the entire surface of the sphere, once the system exceeds the critical radius as \tilde{R} increases.

2 can be changed, while the particle number of component 1 remains constant. The density profile $n = n(\phi, \theta)$ of each component is then obtained by integration along the radial direction \hat{r} for different values of η . Due to the rotational symmetry of the distribution, we rotate the corresponding density matrix so that the center of the density profiles aligns with the north pole of the sphere. The values of the distribution function on any great circles passing through the center point can then be viewed as a function of θ only.

In Fig. 6(a) we numerically present the variation in the angular density profiles of the Bose-Bose mixture for different values of η . All parameters, except for the particle number N_2 of component 2, are consistent with those in Fig. 4(c). The ground-state density profiles of the two components for $\eta = 0.5$ are also shown in Figs. 6(b) and 6(c), respectively. It can be seen that as η decreases, the equilibrium particle-number density of component 1 also decreases, which is qualitatively consistent with the analytical results obtained for the spherical two-dimensional system (Fig. 3). Furthermore, when $\eta = 0.5$ (or 0.4), we observe that $n_1(\theta) - \min[n_1(\theta)]$ closely matches the angular density profile of component 2, $n_2(\theta)$. This suggests that the particles of component 1 can be divided into two parts: The portion denoted by $\min[n_1(\theta)]$ corresponds to a uniformly distributed condensate over the entire spherical surface and the remaining part is then combined with component 2 to form a symmetric quantum droplets as $\{n_1(\theta) - \min[n_1(\theta)]\}/n_2(\theta) \simeq 1$. In this case, the droplet achieves greater stability as $n_2/n_1 \simeq \sqrt{g_{11}/g_{22}}$ is fulfilled, as has been demonstrated both theoretically [7,12] and experimentally [9–11]. Our numerical calculations have thus verified the coexistence of droplet states and uniform condensates in a spherical confinement system.

VI. CONCLUSION

To summarize, we have shown that for a Bose-Bose mixture on a spherical surface with attractive interspecies and repulsive intraspecies interactions, the energy per particle can have a minimum at a finite density after taking the LHY correction into account. This indicates the formation of

liquidlike droplet states of condensates stabilized by quantum fluctuations.

Although in free space droplets with boundaries can always form for given parameters [7,12], in a spherical system, due to its finite area and the presence of curvature, droplet states can only appear within specific parameter ranges and are dependent on the total number of particles as well as

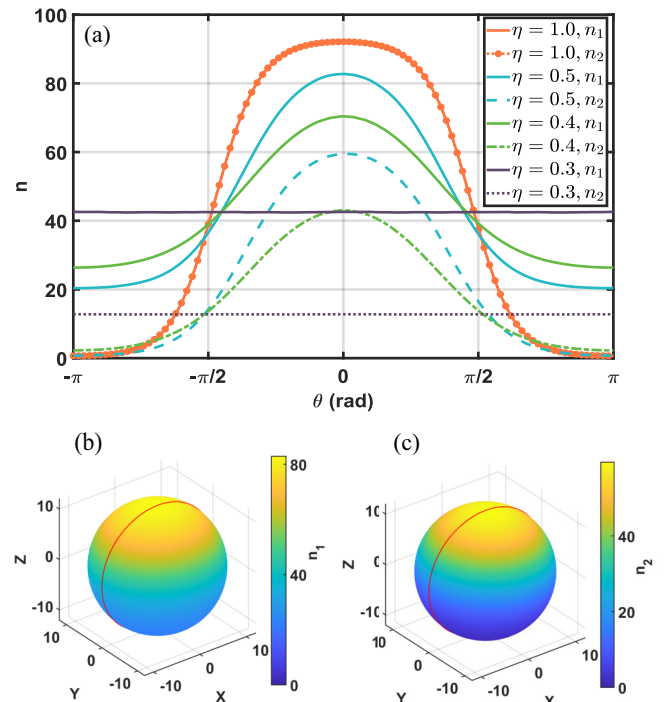


FIG. 6. (a) Variation in the angular density profiles of the Bose-Bose mixture integrated along the radial direction \hat{r} for different values of η . Also shown are the ground-state density profiles of (b) component 1 and (c) component 2 of the Bose-Bose mixture for $\eta = 0.5$. The red curved line in both figures indicates the corresponding spherical cross-sectional line. The other parameters are $N_1 = 0.77N_0$, $N_2 = \eta N_1$, $g_{12} = -1.05$, and $N_0 = 10^5$.

the ratio of particles between components. We numerically found the ground states of the system by solving the extended Gross-Pitaevskii equation using the imaginary-time-evolution method for different parameters, incorporating both bubble traps and an additional repulsive LHY term derived from the Bogoliubov spectrum of a three-dimensional homogeneous mixture. Our findings indicate that the physical behaviors they exhibit are consistent with our theoretical predictions. Meanwhile, the numerical results show that the finite area of the sphere surface also allows for the coexistence of droplet states and uniform condensates. We also emphasize that although our current discussion is limited to the characteristics of the ground state of the system, the dynamic effects of the system during the formation of droplets are another very interesting topic that deserves further in-depth discussion. Our work thus provides inspiration for exploring the potential new forms of droplet states in confined systems.

ACKNOWLEDGMENTS

We thank Professor X.-W. Luo for helpful discussions. This work was funded by National Natural Science Foundation of China (Grants No. 12474366, No. 11974334, and No. 22172151), the Strategic Priority Research Program of the Chinese Academy of Sciences (Grant No. XDB05000000), and the Innovation Program for Quantum Science and Technology (Grants No. 2021ZD0301200 and No. 2021ZD0301500). X.-F.Z. also acknowledges support from CAS Project for Young Scientists in Basic Research (Grant No. YSBR-049).

DATA AVAILABILITY

The data that support the findings of this article are not publicly available. The data are available from the authors upon reasonable request.

[1] T. D. Lee, K. Huang, and C. N. Yang, *Phys. Rev.* **106**, 1135 (1957).

[2] G. E. Astrakharchik, J. Boronat, J. Casulleras, I. L. Kurbakov, and Y. E. Lozovik, *Phys. Rev. A* **79**, 051602(R) (2009).

[3] C. Mora and Y. Castin, *Phys. Rev. Lett.* **102**, 180404 (2009).

[4] V. I. Yukalov and E. P. Yukalova, *Phys. Rev. A* **90**, 013627 (2014).

[5] L. Pitaevskii and S. Stringari, *Bose-Einstein Condensation and Superfluidity* (Oxford University Press, Oxford, 2016).

[6] N. Navon, S. Piatecki, K. Günter, B. Rem, T. C. Nguyen, F. Chevy, W. Krauth, and C. Salomon, *Phys. Rev. Lett.* **107**, 135301 (2011).

[7] D. S. Petrov, *Phys. Rev. Lett.* **115**, 155302 (2015).

[8] C. J. Pethick and H. Smith, *Bose-Einstein Condensation in Dilute Gases* (Cambridge University Press, Cambridge, 2008).

[9] C. R. Cabrera, L. Tanzi, J. Sanz, B. Naylor, P. Thomas, P. Cheiney, and L. Tarruell, *Science* **359**, 301 (2018).

[10] P. Cheiney, C. R. Cabrera, J. Sanz, B. Naylor, L. Tanzi, and L. Tarruell, *Phys. Rev. Lett.* **120**, 135301 (2018).

[11] G. Semeghini, G. Ferioli, L. Masi, C. Mazzinghi, L. Wolswijk, F. Minardi, M. Modugno, G. Modugno, M. Inguscio, and M. Fattori, *Phys. Rev. Lett.* **120**, 235301 (2018).

[12] D. S. Petrov and G. E. Astrakharchik, *Phys. Rev. Lett.* **117**, 100401 (2016).

[13] P. Zin, M. Pylak, T. Wasak, M. Gajda, and Z. Idziaszek, *Phys. Rev. A* **98**, 051603(R) (2018).

[14] H. Hu and X.-J. Liu, *Phys. Rev. Lett.* **125**, 195302 (2020).

[15] P. Zin, M. Pylak, and M. Gajda, *Phys. Rev. A* **106**, 013320 (2022).

[16] X.-F. Zhou, C. Wu, G.-C. Guo, R. Wang, H. Pu, and Z.-W. Zhou, *Phys. Rev. Lett.* **120**, 130402 (2018).

[17] J.-M. Cheng, M. Gong, G.-C. Guo, Z.-W. Zhou, and X.-F. Zhou, *New J. Phys.* **21**, 123051 (2019).

[18] G.-S. Xu, M. Jain, X.-F. Zhou, G.-C. Guo, M. A. Amin, H. Pu, and Z.-W. Zhou, *Phys. Rev. Res.* **6**, 023272 (2024).

[19] C. Lannert, T.-C. Wei, and S. Vishveshwara, *Phys. Rev. A* **75**, 013611 (2007).

[20] K. Sun, K. Padavić, F. Yang, S. Vishveshwara, and C. Lannert, *Phys. Rev. A* **98**, 013609 (2018).

[21] K. Padavić, K. Sun, C. Lannert, and S. Vishveshwara, *Europhys. Lett.* **120**, 20004 (2017).

[22] A. Tononi and L. Salasnich, *Phys. Rev. Lett.* **123**, 160403 (2019).

[23] A. Tononi, F. Cinti, and L. Salasnich, *Phys. Rev. Lett.* **125**, 010402 (2020).

[24] B. Rhyno, N. Lundblad, D. C. Aveline, C. Lannert, and S. Vishveshwara, *Phys. Rev. A* **104**, 063310 (2021).

[25] K. Padavić, K. Sun, C. Lannert, and S. Vishveshwara, *Phys. Rev. A* **102**, 043305 (2020).

[26] O. Zobay and B. M. Garraway, *Phys. Rev. Lett.* **86**, 1195 (2001).

[27] O. Morizot, C. L. G. Alzar, P.-E. Pottie, V. Lorent, and H. Perrin, *J. Phys. B* **40**, 4013 (2007).

[28] O. Zobay and B. M. Garraway, *Phys. Rev. A* **69**, 023605 (2004).

[29] R. A. Carollo, D. C. Aveline, B. Rhyno, S. Vishveshwara, C. Lannert, J. D. Murphree, E. R. Elliott, J. R. Williams, R. J. Thompson, and N. Lundblad, *Nature (London)* **606**, 281 (2022).

[30] Y. Guo, E. M. Gutierrez, D. Rey, T. Badr, A. Perrin, L. Longchambon, V. S. Bagnato, H. Perrin, and R. Dubessy, *New J. Phys.* **24**, 093040 (2022).

[31] F. Jia, Z. Huang, L. Qiu, R. Zhou, Y. Yan, and D. Wang, *Phys. Rev. Lett.* **129**, 243402 (2022).

[32] E. M. Lifshitz and L. P. Pitaevskii, *Statistical Physics: Theory of the Condensed State* (Elsevier, Amsterdam, 2013).

[33] A. Tononi, *Phys. Rev. A* **105**, 023324 (2022).

[34] M. Schick, *Phys. Rev. A* **3**, 1067 (1971).

[35] V. N. Popov, *Theor. Math. Phys.* **11**, 565 (1972).

[36] N. M. Hugenholtz and D. Pines, *Phys. Rev.* **116**, 489 (1959).

[37] A. Tononi, A. Pelster, and L. Salasnich, *Phys. Rev. Res.* **4**, 013122 (2022).

[38] F. Minardi, F. Ancilotto, A. Burchianti, C. D'Errico, C. Fort, and M. Modugno, *Phys. Rev. A* **100**, 063636 (2019).

[39] X. Antoine and R. Duboscq, *Comput. Phys. Commun.* **185**, 2969 (2014).